Investigating the Evolution of Multifragmenting Systems with Fragment Emission Order

E. W. Cornell, T. M. Hamilton, D. Fox,* Y. Lou, and R. T. de Souza
Department of Chemistry and Indiana University Cyclotron Facility, Indiana University, Bloomington, Indiana 47405

M. J. Huang, W. C. Hsi,† C. Schwarz,‡ C. Williams, D. R. Bowman,* J. Dinius, C. K. Gelbke, D. O. Handzy,§ M. A. Lisa,‖ W. G. Lynch, G. F. Peaslee,¶ L. Phair,‖ and M. B. Tsang
National Superconducting Cyclotron Laboratory and Department of Physics and Astronomy, Michigan State University, East Lansing, Michigan 48824

G. VanBuren,** R. J. Charity, and L. G. Sobotka
Department of Chemistry, Washington University, St. Louis, Missouri 63130

W. A. Friedman
Department of Physics, University of Wisconsin, Madison, Wisconsin 53076
(Received 22 May 1996)

Multifragment decays of central collisions in ^{84}Kr + ^{197}Au at $E/A = 70$ MeV are studied. By utilizing a technique sensitive to the emission order of fragments, it is deduced that carbon fragments are emitted prior to beryllium fragments when these fragments have the same velocity. This observation is consistent with the cooling of a thermally decaying source. [S0031-9007(96)01726-7]

PACS numbers: 25.70.Pq, 21.65.+f

Dilute nuclear matter ($\rho/\rho_0 \approx 0.4$) at high temperature ($T = 5-10$ MeV) is predicted to undergo multifragmentation, i.e., decay into a relatively large number of intermediate mass nuclear fragments (IMFs: $3 \leq Z \leq 20$) [1,2]. Experimental observation of large multiplicities of IMFs in both light-ion and heavy-ion induced reactions has been interpreted as multifragment breakup of highly excited, low density nuclear matter [3–7]. Recent experimental results indicate that IMF emission does not occur from a single freeze-out condition [8,9] but rather that IMF emission occurs as the system evolves [10–12]. Whether the decay of the nuclear system is dominated by its collective or thermal properties remains an important open question.

To investigate the general systematics of multifragmentation, we have previously studied the dependence of fragment multiplicity on incident energy for the ^{84}Kr + ^{197}Au system in the range $E/A = 35-400$ MeV [13]. Light charged particles and IMFs produced in the collisions of ^{84}Kr and ^{197}Au nuclei were detected in the angular range $5.4^\circ \leq \theta_{\rm lab} \leq 160^\circ$ by the Michigan State University Miniball/Washington University Miniwall 4π detector array. The absolute energy calibration for this experiment is accurate to 15%. Uncertainties in the relative calibration of beryllium and carbon fragment kinetic energies are estimated to be less than 5%. Experimental details have been previously described [13,14]. To minimize the contribution from emission from multiple sources we have selected central collisions by relating the charged particle multiplicity to an impact parameter scale following a geometrical prescription [15] and gated on large charged particle multiplicity. In this analysis, we have selected events which correspond to $b/b_{\rm max} \leq 0.3$ where $b_{\rm max}$ refers to the maximum interaction radius for which two charged particles are emitted. These central collisions have charged particle multiplicities of $N_{\rm C} \geq 35$ and average IMF multiplicities of $\langle N_{\rm IMF} \rangle \approx 6$ at $E/A = 70$ MeV [13].

The issue of whether thermal or collective (Coulomb, angular momentum, expansion) effects dominate the evolution of the system can be addressed by examining the order of fragment emission. The kinetic energy of fragments emitted from a hot source characterized by a temperature, T, consists of thermal, Coulomb, and perhaps collective terms. If the thermal term dominates, then the average energy for fragments of different mass will be the same. In this case, one expects that as the initially hot system deexcites (cools), at a given instant (temperature) fragments of equal average energy should be emitted. In contrast, if fragment emission is dominated by collective properties of the emitting system, on average fragments with the same velocity will be emitted at the same time.

To investigate the order of fragment emission we probed the Coulomb interaction for pairs of distinguishable fragments (different Z, A, etc.) emitted close to the same direction [16,17] ($\theta_{\rm rel} \leq 20$). If two fragments are emitted with a small relative angle and the first fragment is emitted with a higher velocity than the second fragment, the Coulomb interaction between fragments is weak. On the other hand, when the second fragment has a higher velocity it "catches up" to the first fragment and scatters so that the relative angle between the fragments is increased. In order to study this interaction we have constructed the yield distribution of coincident pairs of light and heavy fragments as a function of their difference velocities ($v_{\rm diff} = |v_{\rm heavy}| - |v_{\rm light}|$) for fragments with small relative final angle.

 0031-9007/96/77(22)/4508(4)$10.00

If the light fragment is emitted first and the heavy fragment has a higher velocity, the final relative angle will be increased. Thus, for fragment pairs with small final relative angle a suppression will be observed for $v_{\mathrm{diff}} \geq 0$. Similarly, if the heavy fragment is emitted first, fragment pairs with $v_{\mathrm{diff}} \leq 0$ are suppressed. In reality, either the light or heavy fragment may be emitted first with some probability. Consequently, as can be seen in Fig. 1, for the correlated fragments a suppression at $v_{\mathrm{diff}} \approx 0$ is evident. The value of v_{diff} at which this suppression is largest is related to the order of fragment emission. For example, if the heavy fragment is emitted first more than 50% of the time, values of $v_{\mathrm{diff}} \leq 0$ will be suppressed more than values of $v_{\mathrm{diff}} \geq 0$, and thus the point of maximum suppression will be shifted to a negative value.

To transform the measured fragment kinetic energies to velocities we have utilized the average mass measured in Silicon-CsI(Tl) telescopes present in the experiment. The threshold for mass identification in these telescopes was $\approx$11 MeV/$\overline{\mathrm{A}}$. The velocities of the fragments were transformed into the center-of-mass assuming $v_{\mathrm{cm}} = 3$ cm/ns. In this analysis, we have focused on IMFs with atomic numbers $Z = 4$ and 6 (Be and C fragments, respectively) emitted close to the same direction in the lab ($|\theta_1 - \theta_2| \leq 10°$, $|\phi_1 - \phi_2| \leq 30°$) and in the angular range $18.75° \leq \theta_{\mathrm{lab}} \leq 50°$.

In Fig. 1 the correlated and uncorrelated v_{diff} distributions are shown. The correlated distribution consists of coincident IMF pairs detected in the angular range previously described. It exhibits a clear suppression of yield for values of v_{diff} close to zero as a result of the Coulomb interaction between the two fragments. The uncorrelated distribution was constructed using IMFs from different events so that it contains all the information about the geometry and velocity distributions, yet none of the correlations present in the true coincidences.

To determine the point of maximum suppression in the v_{diff} distribution we have divided the correlated distribution by the uncorrelated distribution. This ratio is shown as solid points in Fig. 2. For v_{diff} outside the range shown in Fig. 2 the ratio is essentially flat. As expected there is a suppression in this distribution near $v_{\mathrm{diff}} = 0$. The point of maximum suppression can be extracted by fitting the vicinity of $v_{\mathrm{diff}} = 0$ with the function $P(v_{\mathrm{diff}}) = a + b \exp -0.5[(v_{\mathrm{diff}} - c)/d]^2$ in the region $-0.75 \leq v_{\mathrm{diff}} \leq 0.75$. The point of maximum suppression occurs at a negative value of v_{diff} ($v_{\mathrm{diff}} = -0.13 \pm 0.06$ cm/ns) which indicates that on average carbon fragments are emitted before the beryllium fragments. The uncertainty of 0.06 cm/ns is primarily due to the 5% relative uncertainty in the kinetic energy of carbon and beryllium fragments. Uncertainties associated with the fitting procedure are significantly smaller. The quality of the fit achieved is indicated by the thin solid lines visible in Fig. 2. To estimate the fraction of the time the carbon fragments are emitted prior to beryllium fragments we have compared the data with the predictions of a 3-body Coulomb trajectory model. In this model [18], the IMFs are emitted from the surface of a source with $A = 92$, $Z = 40$, and $R = 7$ fm. The relative time between successive IMF emissions was assumed to have an exponential form $[P(t) = \exp(-t/\tau)]$ with a characteristic time $\tau = 75$ fm/c. The ratio of the correlated to uncorrelated v_{diff} distributions from the trajectory calculations are shown as lines in Fig. 2. For the 3-body calculation in which there is no preference for emission order (dotted line) the point of maximum suppression is at zero as expected. For the calculation in which Be fragments are always emitted first the point of maximum suppression shifts to 0.21 cm/ns (solid line). For the calculation in which C fragments are always emitted first the point of maximum suppression shifts to ≈ -0.22 cm/ns

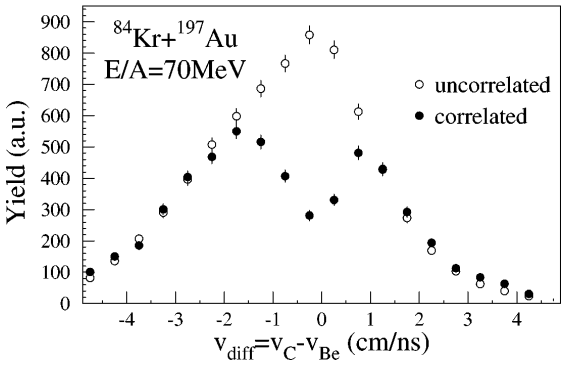

FIG. 1. Difference velocity distributions v_{diff} for Be-C fragment pairs which are correlated (same event) and uncorrelated (different events).

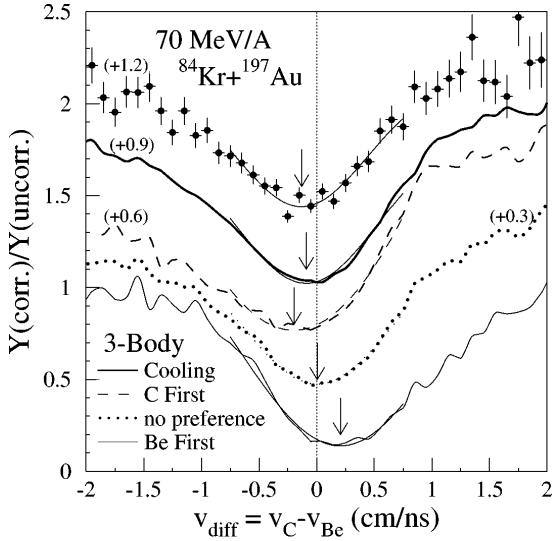

FIG. 2. Ratio of the correlated and the uncorrelated v_{diff} distributions for data (solid points) and 3-body calculations (lines). The point of maximum suppression is indicated by the arrow. For ease of comparison the curves have been vertically offset by the amount indicated in parentheses.

(dashed line). The point of maximum suppression was found to depend linearly on the fraction of the carbon emitted first. By comparing the experimental data with these calculations we find that the C fragment is emitted first 80% ± 14% of the time. We have explored the uncertainties associated with our choice of (Z, A), R, and τ. Our results are summarized in Table I.

To verify that such a time ordering can be explained in terms of cooling of the emitting system by successive emissions, we have performed trajectory calculations with an energy dependent emission time. We have used results from the expanding emitting source (EES) model [10] to determine the dependence of the fragment emission time on energy. The relative emission time distribution for both the carbon and beryllium fragments has been parametrized as $P(t) = e^{-t/\tau}$, where $\tau = 220e^{-E/53}$ (fm/c), and E is the energy of the fragment in MeV. The *calculated* ratio in v_{diff} from this cooling scenario is depicted as a solid line just below the data in Fig. 2. The point of maximum suppression for the trajectory calculation with cooling is at a negative value of −0.08. Comparing the trajectory calculation with cooling to the trajectory calculations without cooling, one deduces that carbon is emitted before beryllium 70% of the time. This result agrees with the value of 80% ± 14% previously determined from the data within the systematic uncertainties.

Shown in Fig. 3 is the two dimensional velocity distribution of carbon and beryllium fragments in the center-of-mass frame. The distribution exhibits a suppression approximately along the line $v_{\mathrm{Be}} = v_{\mathrm{C}}$ since the Coulomb interaction is strongest for fragments of nearly *equal* velocities. The individual carbon and beryllium velocity distributions are peaked at $v = 3.2$ cm/ns and $v = 4$ cm/ns, respectively. The velocities of carbon fragments range from 2.0–4.5 cm/ns while the beryllium fragments are emitted over a broader range (2.0–6.5 cm/ns). We have constructed a time scale for emission of C and Be fragments based upon our earlier exponential parametrization. This scale (denoted by arrows in Fig. 3 shows that for fragments of equal velocity C fragments are on average emitted first.

In order to determine if the difference velocity technique yields time scales consistent with other techniques for extracting the emission time scale, we have constructed

TABLE I. Emission order predicted by the trajectory model for different source characteristics.

Z, A	R	τ	% Carbon first
40,92	7	75	80 ± 14
40,92	7	25	79
40,92	7	150	76
40,92	6	75	70
40,92	8	75	82
30,64	7	75	85
50,118	7	75	69

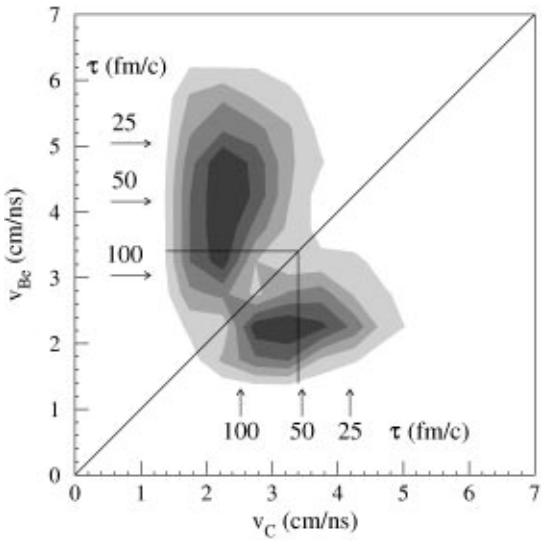

FIG. 3. Linear contour plot of the joint velocity distribution of coincident Be-C fragment pairs. Clear suppression along the line $v_{\mathrm{C}} = v_{\mathrm{Be}}$ is evident due to the Coulomb repulsion between fragments.

relative velocity correlation functions [18–26] for pairs of Be and pairs of C fragments.

$$1 + R(v_{\mathrm{red}}) = \frac{Y_{12}(v_1, v_2) \int Y_1 Y_2}{[Y_1(v_1) * Y_2(v_2)] \int Y_{12}}$$

$$v_{\mathrm{red}} = |v_1 - v_2|/\sqrt{Z_1 + Z_2}$$

where Y_1 and Y_2 represent the uncorrelated yield for fragments 1 and 2, respectively, and Y_{12} represents the correlated yield. The results of this analysis are shown in Fig. 4 as solid points. To avoid uncertainties associated with near Coulomb barrier emission, we have selected fragment pairs with velocities $v_{\mathrm{min}} = 3.4$ cm/ns. The quantity v_{min} is the velocity of the less energetic fragment in

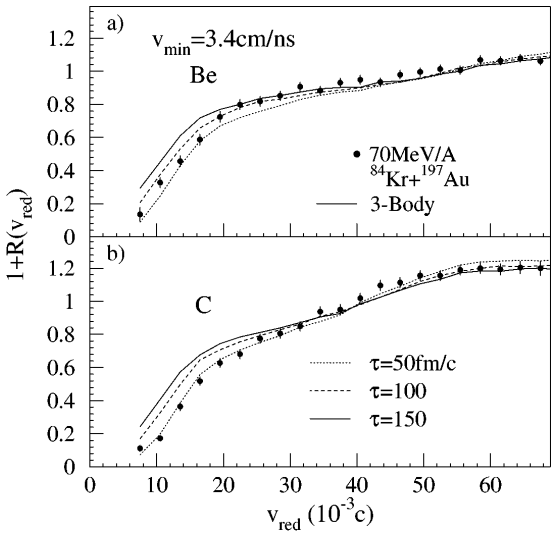

FIG. 4. Reduced velocity correlation functions for Be-Be pairs and C-C pairs [panels (a) and (b), respectively].

the pair. We have used this same v_{min} cut for both Be and C fragments since our v_{diff} analysis intrinsically selects fragments of the same velocity. The correlation function shown in Fig. 4 shows a suppression for small values of v_{red} ($\leq 0.03c$). This suppression is primarily due to the Coulomb repulsion between the fragments in the pair and provides a measure of the spatial and temporal size of the emitting source. Fragments emitted from a small source (or with a short mean emission time) manifest a stronger Coulomb interaction than fragments emitted from a larger source (or with a longer mean emission time). An increase in the strength of the Coulomb interaction is manifested as a suppression in the correlation function over a larger v_{red} range. The width of the suppression in the correlation function can be related to the spatial-temporal extent of the emitting source.

In order to extract approximate time scales, we have compared the data to the predictions of a 3-body Coulomb trajectory model [11]. The predictions of this model are shown as lines in Fig. 4. The same initial source mass, charge, and radius parameters were chosen as described in the calculations for Fig. 2. The emission was assumed to be described by an exponential $P(t) = \exp(-t/\tau)$ characterized by an emission time constant τ. Calculations were performed for mean emission times of $\tau = 50$, 100, and 150 fm/c. Comparison of the experimental data in Fig. 4 with the model predictions indicates that the time scale for the $Z = 4$ fragments is slightly less than 100 fm/c. The extracted time scale for $Z = 6$ fragments, however, is approximately 50 fm/c. These results are consistent with the exponential parametrization of the emission time scale and the v_{diff} analysis. The extracted emission times for $v_{min} = 3.4$ cm/ns imply the same emission order as observed in the v_{diff} analysis.

In summary, we have investigated the relative emission order for beryllium and carbon fragments in the reaction ^{84}Kr + ^{197}Au at $E_{lab}/A = 70$ MeV using difference velocity distributions. The experimental data indicates that for fragments of nearly equal velocity carbon fragments are emitted prior to beryllium fragments $\approx$80% of the time. This apparent ordering of fragments can be reproduced by a 3-body Coulomb trajectory model which incorporates cooling as the source emits. The fragment emission order was compared to the time scale for emission of carbon and beryllium fragments based on relative velocity correlation functions. The values of $\tau_{Be} \approx 100$ fm/c and $\tau_C \approx 50$ fm/c which the relative velocity correlation functions yield are qualitatively consistent with the relative emission order analysis. Apparent emission ordering of fragments is a consequence of the selection of near equal velocity fragments by the Coulomb interaction. Both of these results are consistent with the logarithm of the fragment emission time being roughly proportional to the fragment energy. This observation can be understood as the cooling of a thermally decaying source.

We would like to acknowledge the valuable assistance of the staff and operating personnel of the K1200 Cyclotron at Michigan State University for providing the high quality beams which made this experiment possible. One of the authors (R. D.) gratefully acknowledges the support of the Sloan Foundation through the A. P. Sloan Fellowship program. This work was supported by the U.S. Department of Energy under DE-FG02-92ER40714 (Indiana University) and DE-FG02-87ER-40316 (Washington University) and the National Science Foundation under Grants No. PHY-90-15957, No. PHY-93-14131, and No. PHY-92-14992 (Michigan State).

*Present address: CRL, Chalk River, Ontario K0J 1J0, Canada.
†Present address: IUCF, Bloomington, Indiana 47405.
‡Present address: GSI, D-64220, Darmstadt, Germany.
§Present address: Deloitte and Touche Consulting Group, 2 World Financial Center, New York, NY 10281.
‖Present address: LBL, University of California, Berkeley, CA 94720.
¶Present address: Department of Chemistry, Hope College, Holland, MI 49423.
**Present address: Department of Physics, MIT, Cambridge, MA 02139.

[1] G. Bertsch and P. J. Siemens, Phys. Lett. **126B**, 9 (1983).
[2] W. Bauer *et al.*, Phys. Rev. Lett. **58**, 863 (1987).
[3] J. E. Finn *et al.*, Phys. Rev. Lett. **49**, 1321 (1982).
[4] J. W. Harris *et al.*, Nucl. Phys. **A471**, 241c (1987).
[5] C. A. Ogilvie *et al.*, Phys. Rev. Lett. **67**, 1214 (1991).
[6] R. T. de Souza *et al.*, Phys. Lett. B **268**, 6 (1991).
[7] D. R. Bowman *et al.*, Phys. Rev. Lett. **67**, 1527 (1991).
[8] J. Bondorf *et al.*, Nucl. Phys. **A444**, 460 (1985).
[9] D. H. E. Gross *et al.*, Phys. Rev. Lett. **56**, 1544 (1986).
[10] W. A. Friedman, Phys. Rev. C **42**, 667 (1990).
[11] E. Cornell *et al.*, Phys. Rev. Lett. **75**, 1475 (1995).
[12] T. M. Hamilton *et al.*, Phys. Rev. C **53**, 2273 (1996).
[13] G. F. Peaslee *et al.*, Phys. Rev. C **49**, R2271 (1994).
[14] R. T. de Souza *et al.*, Nucl. Instrum. Methods Phys. Res., Sect. A **295**, 109 (1990).
[15] C. Cavata *et al.*, Phys. Rev. C **42**, 1760 (1990).
[16] C. J. Gelderloos and J. M. Alexander, Nucl. Instrum. Methods Phys. Res., Sect. A **349**, 618 (1994).
[17] C. J. Gelderloos *et al.*, Phys. Rev. Lett. **75**, 3082 (1995).
[18] Y. D. Kim *et al.*, Phys. Rev. C **45**, 338 (1992).
[19] R. Trockel *et al.*, Phys. Rev. Lett. **59**, 2844 (1987).
[20] Y. D. Kim *et al.*, Phys. Rev. Lett. **67**, 14 (1991).
[21] D. Fox *et al.*, Phys. Rev. C **47**, R421 (1993).
[22] E. Bauge *et al.*, Phys. Rev. Lett. **70**, 3705 (1993).
[23] T. C. Sangster *et al.*, Phys. Rev. C **47**, R2457 (1993).
[24] D. Fox *et al.*, Phys. Rev. C **50**, 2424 (1994).
[25] T. Glasmacher *et al.*, Phys. Rev. C **50**, 952 (1994).
[26] R. Bougault *et al.*, Phys. Lett. B **232**, 291 (1989).